Bulletin of the Mineral Research and Exploration

http://bulletin.mta.gov.tr

Geology of the Yeşilyurt gold deposit: an example of low-angle normal fault related mineralization, Eastern Anatolia-Turkey

Esra YILDIRIM[a*], Nail YILDIRIM[b], Cahit DÖNMEZ[c] and Kurtuluş GÜNAY[d]

[a]*Fırat University, Department of Geological Engineering, Elazığ 23000, Turkey*
[b]*IV. Regional Directorate of Mineral Research and Exploration, Malatya 44100,Turkey*
[c]*General Directorate of Mineral Research and Exploration, Ankara 06800, Turkey*
[d]*Marmara Regional Directorate of Mineral Research and Exploration, Kocaeli, Turkey*

Research Article

Keywords:
Yeşilyurt gold mineralization, Detachment fault/Low-angle normal fault, Fault gauge, Cataclasite, Breccia.

ABSTRACT

Yeşilyurt gold mineralization is located within the provincial borders of Malatya and Adıyaman in the East Anatolian Region. This mineralization is one of the gold deposits which correlated with low-angle normal/detachment fault. Low-angle normal fault associated with a tectonic setting which is potential extensional in Paleogene-Neogene (?) term. Marble-recrystallized limestone which belongs to the metamorphic core is the dominant rock (footwall) type in the bottom plate of the fault zone. There are deformed graphitic calc-schists (hanging wall) in the upper plate of the fault zone. The fault zone is characterized by fault gauge, cataclasite, and breccia. While the cataclasite, and breccia are the principal ore host, there is weaker mineralization in fault gauge. Alteration assemblages are: (1) silica replacements/veinlets and, (2) quartz-pyrite replacements / veinlets. High gold contents are closely related to silicification and quartz-pyrite alteration which damaged the primary textures. Small volume syn-tectonic magmatic rocks are simultaneous and typically monitored in the silicified areas which are border on the high-grade gold mineralization. Mineralization is a non-base metalliferous Au depositthat contains Au/Ag ~ 1.07, As (~0.27%), F (1.59%), and a trace amount of Sb. This deposit will lead to finding new gold deposits in Eastern Taurus Orogenic Belt.

Received Date: 29.07.2020
Accepted Date: 20.09.2020

1. Introduction

The mineralization area is located in the Eastern Taurus Orogenic Belt which is the part of the Alpine-Himalayan metallogenic belt, and covers the Malatya-Yeşilyurt and Adıyaman-Çelikhan region (Figure 1). This belt is one of the most important provinces in terms of mining regions. It contains different types of deposits such as; volcanogenic massive sulfide, epithermal, iron-oxide-Cu-Au (IOCG), skarn, and porphyry (Cu-Mo). Several academic studies and mining activities have been mostly focused on IOCG deposits (Helvacı and Griffin, 1984; Yılmazer et al., 2003; Kuşcu et al., 2007, 2013; Çelebi, 2009), skarn deposits (Yılmaz et al., 1992; Yiğit, 2009; Kuşcu et al., 2010; Kalender, 2011; Hanelçi and Çelebi, 2013; Öztürk et al., 2019; Yıldırım et al., 2019), epithermal / porphyry deposits (Dumanlılar et al., 1999; Altman and Liskovich, 2011; İmer et al., 2012) and volcanogenic massive sulfide deposits (Şaşmaz et al., 1999; Akıncı, 2009; Yıldırım et al., 2012; Yıldırım, 2013; Yıldırım et al., 2016) because of their economic importance.

Citation Info: Yıldırım, E., Yıldırım, N., Dönmez, C., Günay, K. 2021. Geology of the Yeşilyurt gold deposit: an example of low-angle normal fault related mineralization, Eastern Anatolia-Turkey.Bulletin of the Mineral Research and Exploration 164, 261-279. https://doi.org/10.19111/bulletinofmre.797729

**Corresponding author: Esra YILDIRIM, eozyildirim@gmail.com*

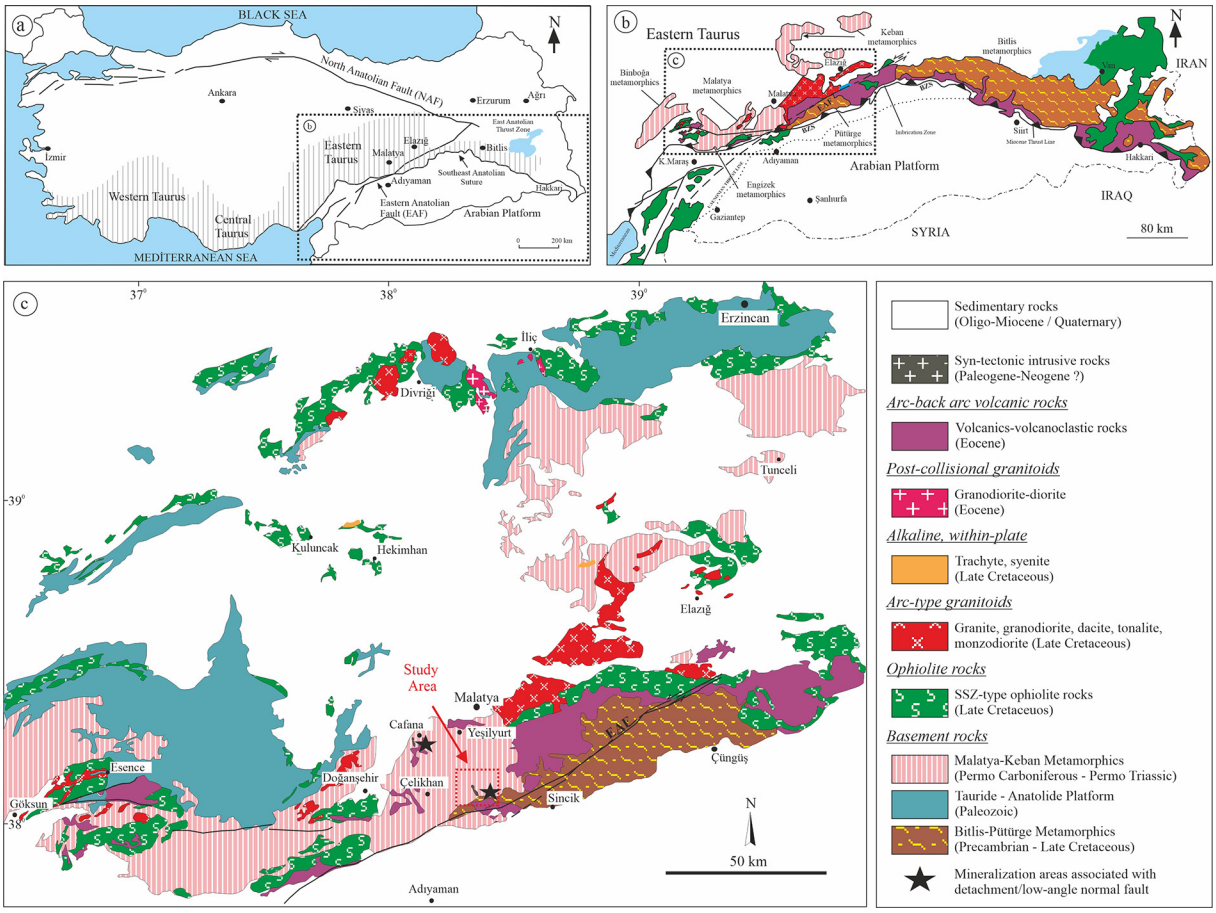

Figure 1- a) The location of the Taurus mountains and some of the main tectonic structures in Turkey, b) simplified geological map showing the main rock units of Eastern Taurus orogenic belt (MTA, 2002), c) mineralizations in the Eastern Taurus orogenic belt associated with large magmatic rock units (MTA, 2002; modified from Yıldırım et al., 2019)

In spite of these studies, low-angle normal fault/ detachment fault systems and development of the ore deposits related to this system in the metamorphic core complexes, have not been reported before.

Although the mineralizations associated with low-angle normal fault or detachment fault have been mined since the 1860s, it has recently been defined as a different deposit type (Long, 1992). These deposits differ significantly from epithermal deposits with their characteristic mineral assemblages, alteration types, ore fluid types, and structural controls, and they are not well known. The model of this type of deposit has not yet been fully investigated and has so far been mostly described in West-Central Arizona, SE California, and the southern margins of Nevada (Long, 1992).

Detachment faults are regional-scale low angle (> 30) normal faults that cause significant regional extension as the footwall (sub-plate) moves upward, generating displacements over tens of kilometers. Mineralization models associated with detachment faults include Fe and Cu oxide replacements, occasionally abundant sulfides in stockworks and veins, as well as barite and/or fluorite veins and Mn oxide veins (Spencer and Welty, 1986; Long, 1992). The fluid might be triggered by heat from either subplate rocks or syn-tectonic magmatic rocks ranging from micro-diorite to rhyolite (Reynolds and Lister, 1987; Long, 1992).

Yeşilyurt gold mineralization is one of the newly defined gold deposit group in the Eastern Taurus Orogenic Belt. Mineralization is located in the south of Malatya province and is 45 km away from the city (Figure 1b-c). Since this mineralization observed in the Eastern Taurus orogenic belt is important in terms of gold and fluorite, it has been the subject of some research studies (Revan and Genç, 2003; Şaşmaz et al., 2005; Altuncu, 2009). From previous studies, Şaşmaz et

al. (2005) have stated that fluorite-gold mineralizations might have occurred at low temperature, high fO_2 and hydrothermal conditions where there is no evidence of magmatic intrusion; Revan and Genç (2003) have claimed that it is strata-bound mineralization that is dependent on paleo-karstification processes and controlled by the dispersed Carboniferous-Permian discordance plane; Altuncu (2009) has argued that it is associated with a hydrothermal replacement type and a buried alkali magmatic mass. Previous studies contain some contradictory data. The types of structures in the metamorphic core complex could not be distinguished, and also the source of the hydrothermal solution is controversial.

The area was re-evaluated after prospecting and detailed exploration studies by MTA (General Directorate of Mineral Research and Exploration). In the field of gold mineralization in Yeşilyurt, the depth (0-115m) dimension of the mineralization was investigated for the first time with the drilling activities (mean depth 140 m; total core drilling 11,000 m) carried out by MTA, and 1,900,000 tons of gold resources with 1 g/ton of Au grade were estimated by using 0.4 g/ton cut-off grade over the field (Yıldırım et al., 2019). The mineralization has been interpreted as a deposit associated with a regional low-angle normal fault within the metamorphic complex.

This study aims to (I) describe and expand the typology of the gold deposit associated with the low-angle normal fault developed in the extensional environment and (II) propose a new regional metallogenic model by focusing on the existence of potential mineralization areas controlled by low-angle normal faulting. To achieve these goals, is we tried to associate the results obtained from geology, structure, types of alteration, geochemistry, textural and mineralogical properties of gold mineralization to low-angle normal fault.

2. Geological Setting

2.1. Regional Geology

The geology and geodynamic evolution of the region should be well known to understand the mineralization and alterations associated with the low-angle normal fault within the metamorphic core complex in the study area located on the border of Malatya-Yeşilyurt and Adıyaman-Çelikhan.

Millions of years of complex geological movements have shaped the region called Turkey's Anatolia (Asia Minor). Turkey is a geologic part of the Alpine-Himalayan belt, also known as the Tethyan belt extending from the Atlantic Ocean to the Himalayas, apart from the small part of the country which is the continuation of the Arab platform located along the Syrian border. The Anatolian peninsula, which has an important place in the Alpine-Himalayan orogenic system, contains the remains of the Tethys (Paleo-Tethys and Neo-Tethys) oceanic basins between approximately E-W trending tectonic belts (Pontides, Anatolides, Taurides, and Margin Folds) (Şengör and Yılmaz, 1981; Ketin, 1983; Okay, 2008; Robertson et al., 2016*a, b*).

The mineralization area in the Eastern Taurids part of the Alp-Himalayan orogenic belt contains many important tectonostratigraphic/tectono-magmatic units (Figure 1b-c) and it has been affected by intensive fracturing, folding, thrusting, and nappe movements. The region includes Permo-Triassic metamorphic rocks, continental-arc, post-collision, intra-plate magmatites, back-arc basin products, and supra-subduction ophiolitic basement rocks (Figure 1c). These units are covered by Paleogene-Neogene (?) sedimentary, volcano-sedimentary, and volcanic rocks. The mineralization area is represented by Precambrian-Paleozoic Pütürge Metamorphics, Late Devonian-Late Cretaceous Bodrum nappe (Bedi and Yusufoğlu, 2018), Devonian-Cretaceous Yahyalı nappe units (Bedi and Yusufoğlu, 2018), and Early-middle Eocene Maden Group units (Figure 2).

Gold mineralizations that may create economic potential are within the metamorphic rocks of the metamorphic core complex (Figure 2). The metamorphic complex consists of marble, recrystallized limestone/dolomitic limestone, mica-schist, calc-schist, and these rocks metamorphosed under low temperature-low pressure conditions. These rocks largely outcrop in the south-southwest of Malatya province and have been identified as Permo-Carboniferous Malatya Metamorphics in previous studies. Some researchers (Asutay et al., 1986; Yılmaz et al., 1992) have considered Malatya Metamorphics as the equivalent of Keban Metamorphics and as their southerly extension (Figure 1c). According to the ages suggested by different researchers (Özgül, 1976; Kipman, 1981; Asutay et al., 1986), Keban Metamorphics are platform-type continental shelf sediments that

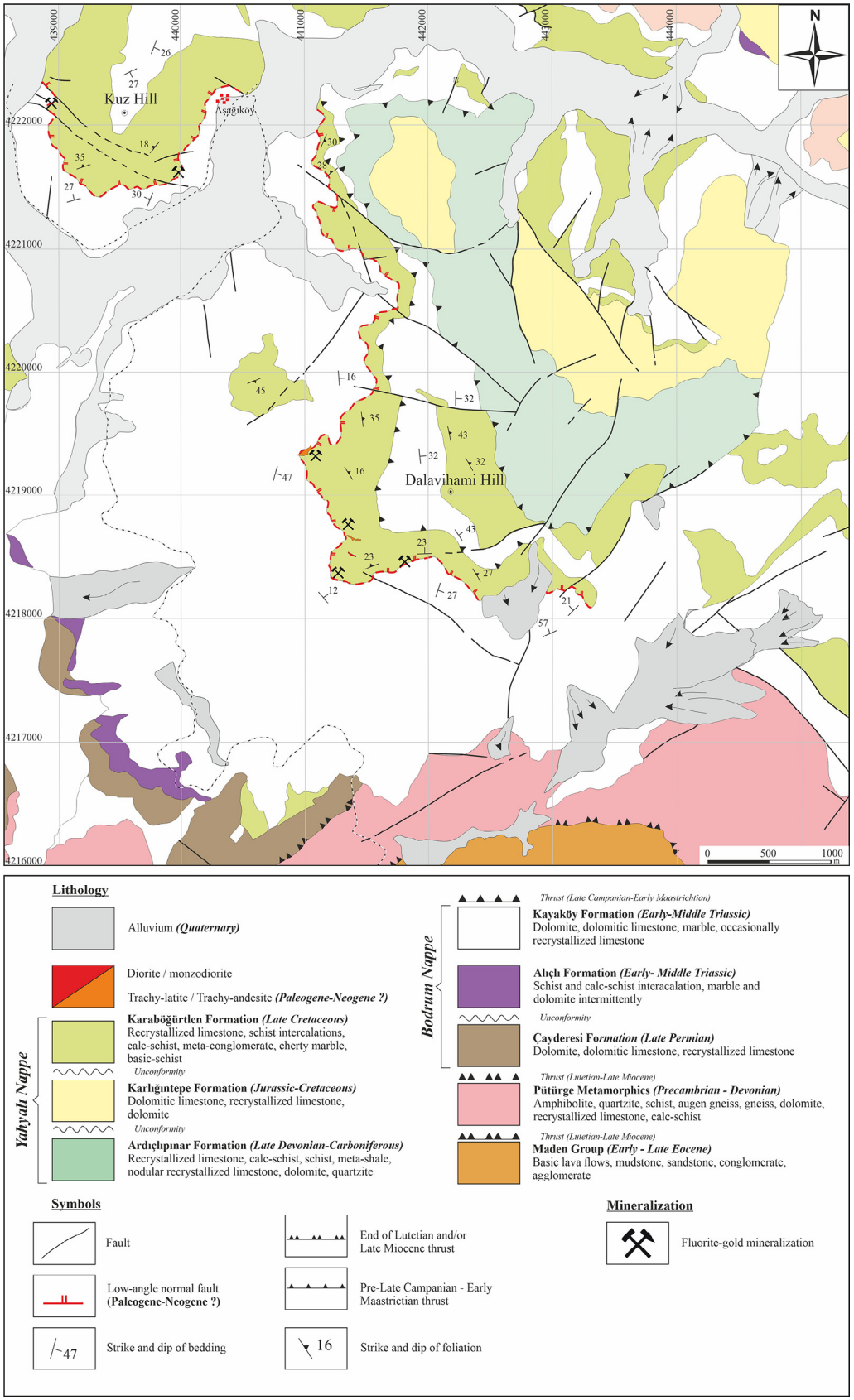

Figure 2- Geological map showing the mineralization in the study area and surroundings (modified from Bedi and Yusufoğlu, 2018).

have undergone a deposition phase started during the Permo-Carboniferous and continued until the Triassic age.

2.2. Geology of the Mineralization Area

Yeşilyurt gold mineralization is observed as tabular bodies along the low-angle normal fault zone developed in Paleogene-Neogene , within the Late Triassic-Late Cretaceous metamorphic rocks. The slickenside of the fault zone is observed as a non-mineralized fault gauge. The hanging wall of the fault zone is a deformed graphite calc-schist of the metamorphic core complex and the footwall is composed of marble (Figures 3 and 4).

Precambrian-Paleozoic-Mesozoic and Cenozoic litho-stratigraphic units have been distinguished in the mineralization area and around. Structurally, from bottom to top and from south to north, respectively; the Late Devonian-Late Cretaceous Bodrum nappe tectonically overlies the Precambrian-Devonian aged Pütürge metamorphics nappe and the Maden Group consisting of volcanic and sedimentary rocks which unconformably overlie the Precambrian-Devonian aged Pütürge metamorphic nappe (Figure 2). The metamorphic units of the Bodrum and Yahyalı nappe have been stated as lower lithological units (such as Kalecik marble, Düzağaç schists, Kerbelek limestone, Koltik formation, Pınarbaşı formation) within the Malatya metamorphics (Gözübol and Önal, 1986; Revan and Genç, 2003; Şaşmaz et al., 2005; Altuncu, 2009). Kayaköy and Karaböğürtlen formations of the Bodrum nappe were cut cross by Paleogene-Neogene igneous rocks as sills and dykes. Quaternary sediments composing of alluvium, alluvial fan, and talus are found at the top of the section in the region. The geological features of metamorphic and igneous rocks hosting the mineralization are given below.

2.2.1. Kayaköy Formation

This formation is observed as the footwall of the low-angle normal fault zone. Dolomite and dolomitic limestones containing recrystallized limestone/ marble intercalations form the dominant lithology. Recrystallized limestone and marbles exposed to

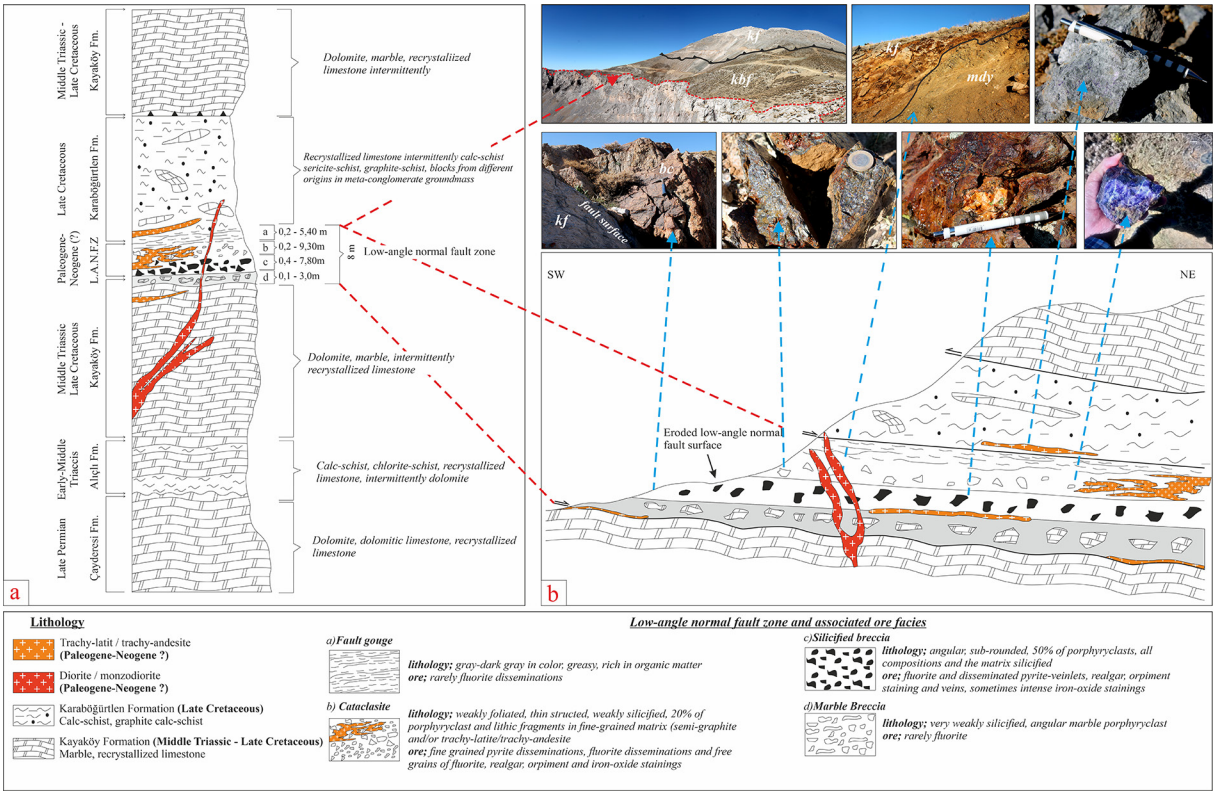

Figure 3- a) Generalized columnar section of the low angle fault zone and main rocks in Yeşilyurt gold mineralizations, b) NE-SW schematic cross-section (unscaled) of the ore sequence and low angle fault zone and associated ore facies (bş: breccia kf: Kayaköy formation, kbf : Karaböğürtlen formation, mdy: monzo-diorite).

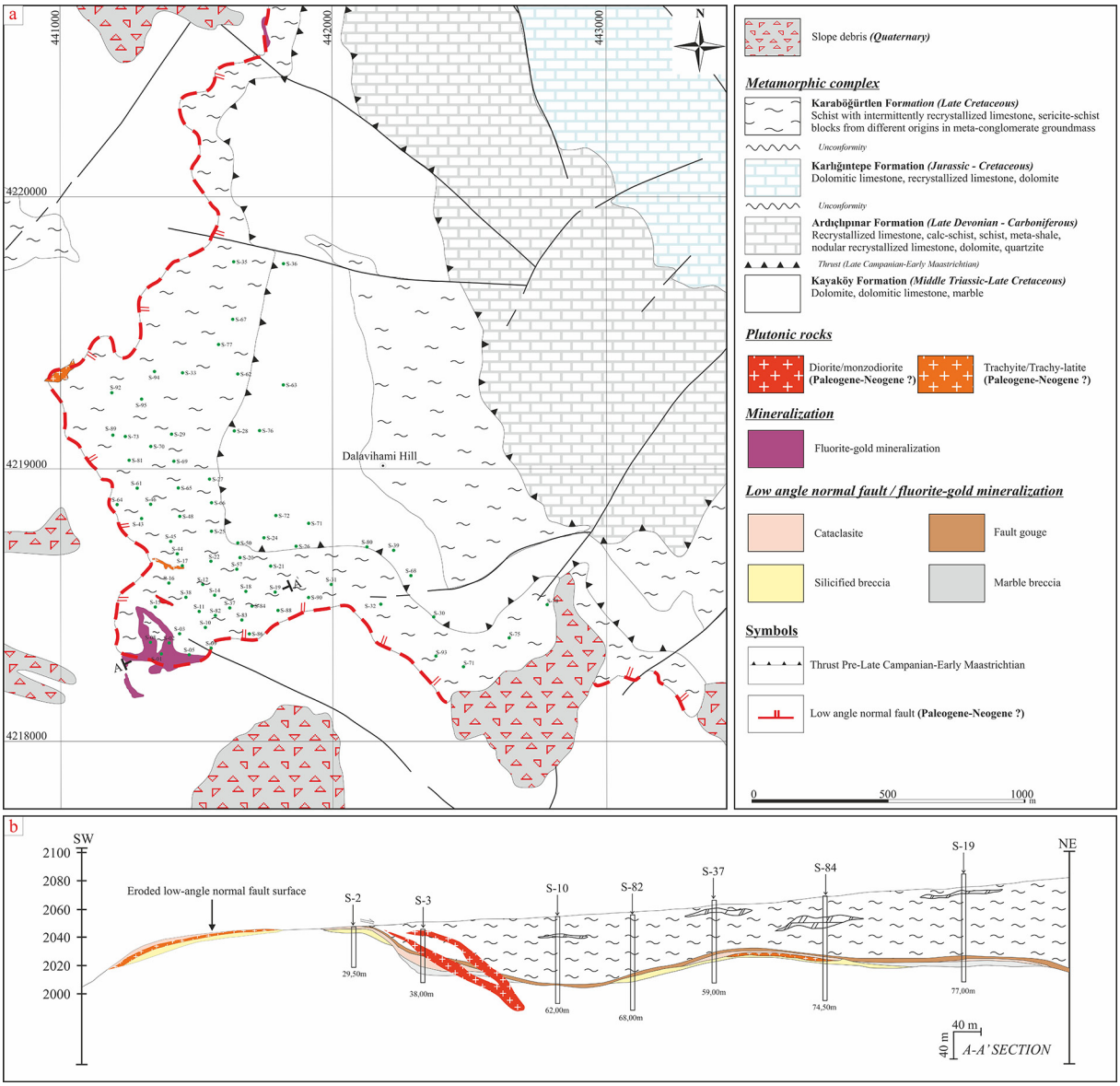

Figure 4- a) Detailed geological map of Yeşilyurt gold mineralization (modified from Bedi and Yusufoğlu, 2018), b) geological cross-section (drilling profiles showing vertical distribution of the ore zone; drilling well locations (from Yıldırım et al., 2019).

structural deformation and hydrothermal alteration host gold mineralization (Figure 3 and 4). The strikes and dips of the limestones appear to be approximately parallel to the low-angle normal fault zone (Figure 2).

2.2.2. Karaböğürtlen Formation

This formation is observed as a hanging wall of the low-angle normal fault zone, which consists of recrystallized limestone, dolomite, and graphite-calc-schists with cherty marble intercalations. In the study area, primarily overlies Middle Triassic-Late Cretaceous Kayaköy formation with an angular unconformity and it is also possible to observe normal and reverse fault relationships with this unit (Figure 3 and 4). The strikes and dips of the limestones and the foliations in the schists appear to be consistent with the low-angle normal fault zone (Figure 2). Even though the foliations of the schists, which have been deformed, were distorted and rotated, they are generally parallel to the fault zone.

2.2.3. Paleogene-Neogene Magmatic Rocks

The magmatic rocks were determined for the first time in the study area and their surroundings are mostly

sills and dykes. The magmatic rocks are composed of sub-volcanic (trachy-latite/trachy-andesite) and intrusive (monzo-diorite, diorite) compositions with textures ranging from aphanitic to porphyry. While trachy-latite/trachy-andesite sills and dykes constitute the magmatic rock type related to mineralization, they mostly occur in ore zones, and generally as laminated flows in schist breccias (Figure 3 and 4). Magmatic rocks are common through in breccias and cataclasites (predominantly as a clast) between Late Triassic-Late Cretaceous Kayaköy and Karaböğürtlen formations along with the NW-SE striking and NE-dipping low-angle normal fault, however, there is no any evidence indicating a cross-cutting relationship with the fault gauge. They have been observed as clast and/or sills up to several meters in thickness within breccia and cataclasites developed along the fault zone during drillings (Figure 3 and 4). Since the recrystallized limestones of the Kayaköy formation behave in basic composition, they have been able to form a weak (30-50 cm) baked zone through the contacts.

Trachy-latite/trachy-andesites are composed of feldspar, hornblende and biotite. Feldspar phenocrystals are distinguished from cataclasite and breccias by alterations such as carbonization, sericitization, and opacitization (Figure 5a) and the presence of biotite and hornblende (Figure 5a-c). The type of plagioclases could not be determined because the trachy-latite/trachy-andesite samples are heavily

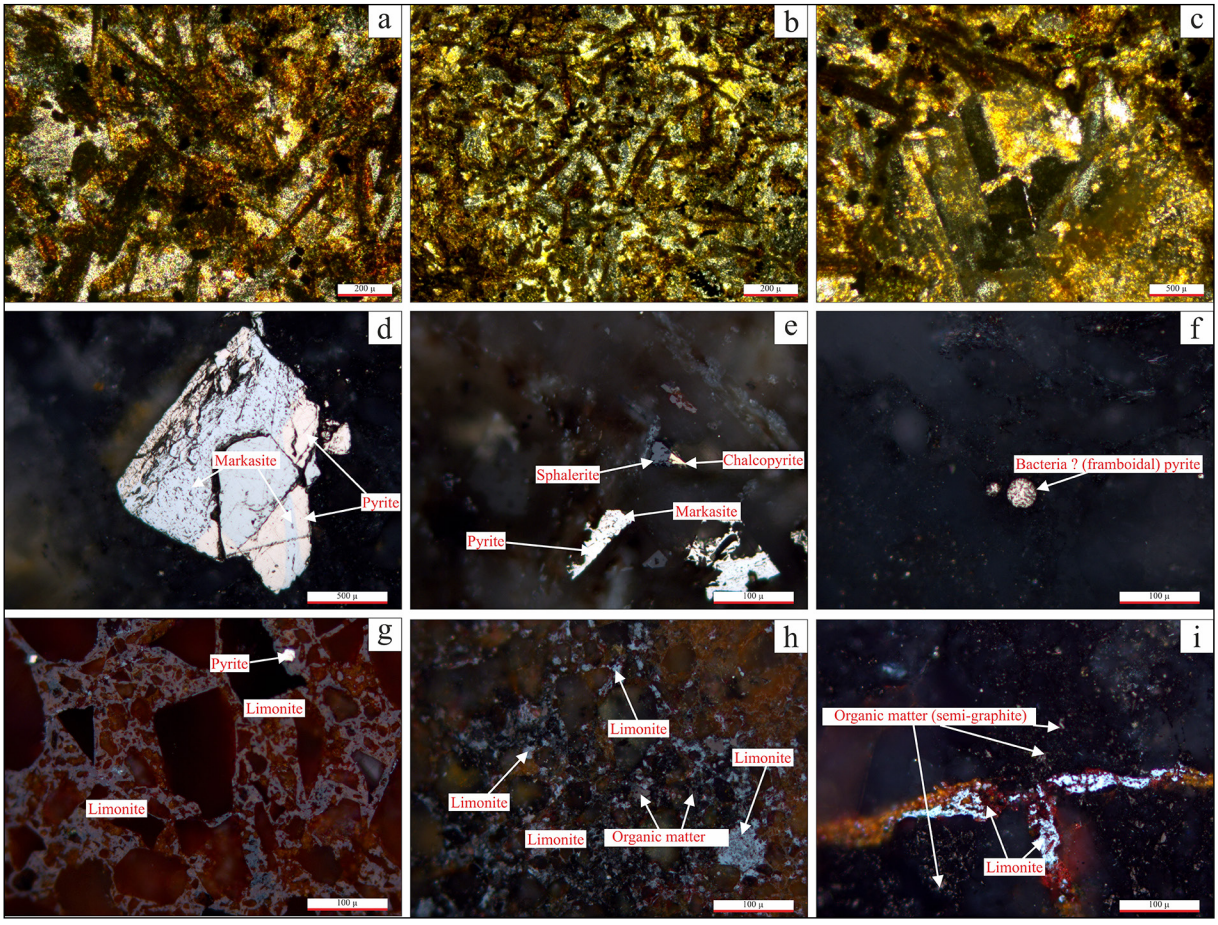

Figure 5- Mineralization views through low angle normal fault (detachment fault) zone in the Yeşilyurt gold mineralizations. a) non-mineralized fault gauge, b) quartz-fluorite in the form of free-space filling in the mineralized cataclasite zone and limonite in fracture fillings (transformation from pyrite), c) Laminated flows through schist breccias in trachy-latite contact, quartz-orpiment-fluorite in the form of space-filling, d) Iron-oxide staining through trachy-latite/organic matter matrix in cataclasites, e) contact between silicified breccia and trachy-latite and widespread iron-oxide staining, f) widespread silicification through breccias, g) the relationship between silicified breccia and trachy-latite, showing syn-genetic mineralization, h) non-mineralized marble breccia, i-j) widespread orpiment in the form of fracture filling and staining and widespread fluorite with open-space filling, k) cataclasite and l) trachy-latites cutting cross silicified breccias

altered. Plagioclases are located in the groundmass as small microlites (Figure 5b). Sericitization and carbonization are common. Hornblende minerals are generally subhedral or euhedral (Figure 5a-c). They are green-dark green, brown under plane-polarized light and they show pleochroism. Usually, prismatic crystals have cleavage in one direction and lozenge-shaped ones have distinct cleavage in two directions. Biotite minerals are generally in the form of opacified thin rod-like crystals and they are subhedral (Figure 5a-c). They appear in colors ranging from light brown to dark brown under plane-polarized light, and dark brown under cross-polarized light. While microlithic texture formed by mostly small crystals (Figure 5b) is observed in trachytes, microporphyritic texture in which sanidine phenocrystals are located in fine-grained groundmass is observed in some of the samples (Figure 5c). Based on the core samples obtained from the drillings, it has been observed that magmatic rocks are widely carbonated, sericitized, opacified, silicified and have disseminated in pyrite up to 2 % and they contain fluorite. The similar alteration of these rocks and mineralized areas and their presence in the mineralization area strongly reveal the direct genetic relationship of trachy-latite / trachy-andesites with the gold deposit. The composition, stratigraphic and structural positions and mineralization associations of the magmatites (Sağıroğlu, 1988; Kalender et al., 2009) defined in the Cafana Pb-Zn ore deposit (Figure 1c) located approximately 25 km northwest of the study area are similar to magmatic rocks in the Yeşilyurt gold mineralization area and they can be correlated. Although there is no available age data for these rocks, structural and stratigraphic positions and ore associations of those suggest that they may be of Paleogene-Neogene(?) age.

Diorite/monzodiorites are mostly in the form of dykes cutting-cross the Karaböğürtlen and Kayaköy formations (Figure 3 and 4). They include feldspar, plagioclase, amphibole, biotite, and opaque minerals and, also arenization is common. These rocks also cut-cross the low-angle normal fault plane (Figure 3 and 4b) and are younger than trachy-latites/trachy-andesites and are not thought to be associated with gold mineralization.

2.3. Structural Geology

The low-angle normal fault, between the Late Cretaceous-Late Triassic aged Kayaköy and Karaböğürtlen formations of the Bodrum nappe, defined for the first time in the mineralization area has continuity for kilometers (> 10 km) and has a slope of about 10° (Figure 2, 3). In the previous studies, this fault has been interpreted and mapped either as unconformity (Revan and Genç, 2003; Bedi and Yusufoğlu, 2018) or reverse fault (Şaşmaz et al., 2005; Altuncu, 2009). A recently defined low-angle normal fault is thought to be reactivated due to Paleogene-Neogene(?) extensional tectonism after the thrust faults previously developed within the metamorphic core complex (Figure 3b). In the mineralization area, syn-tectonic magmatic rocks (trachy-latite/trachy-andesite) have developed along the low-angle normal fault.

Mineralization has developed between the graphite-calc-schist forming the hanging wall and the marbles of the footwall of the low-angle normal fault. This fault zone is composed of three structural units: (1) fault gauge, (2) cataclasite, and (3) breccia zone. While cataclasite and breccia units are the main hosts of the ore, mineralization in the fault gauge is very weak (Figure 3a-b).

Fault gauge: This zone separates the graphitic calc-schists from the underlying marbles. The fault gauge thickens and thins along the plane, indicating a low-angle normal fault zone (Figure 3a). The gauge is averagely 2 meters thick and has probably formed during displacement along the fault, mostly by excessive reduction of grain size of the overlying graphitic-calc-schists and much less underlying marble breccias. Cataclasite, trachy-latite/trachy-andesite, and breccia levels are present in the lower parts of the fault gauge (Figure 3a-b). The fault gauge is rich in organic matter (semi-graphite) and greasy, gray-dark gray. It rarely contains fluorite.

Cataclasite: It is the zone where mineralization is intensely observed and has an average thickness of 2.50 m (Figure 3a). Cataclasites are observed as weakly-foliated, thin structured, greasy and they contain porphyriclasts (calc-schist, quartz, and very little marble) and lytic fragments ranging from <1 mm to 10 mm in size within the fine-grained matrix (rich in organic matter) having generally similar compositions (Figure 3a-b). The lineation along porphyriclasts is notable. The matrix contains very fine-grained quartz, carbonate, and fluorite, and has sometimes iron-

oxide staining. While the grain size and abundance decrease towards the fault gauge, they increase towards the underlying breccia zone. Deformation is more dominant than brittle behavior. Cataclasites are generally mineralized because they present suitable environments for fluid flow and contain fine-grained pyrite disseminations and sequences, fluorite dissemination and veinlets, and also realgar-orpiment (Figure 3b). Silicification is more common in the levels close to the underlying breccia zone.

Breccia: The silicified breccia zone underlying the cataclasites represents the lower part of the fault and is approximately 2.50 m in thickness (Figure 3a). While the upper part is rich in fine-grained matrix and schist fragments, it consists of angular, sub-rounded marble fragments towards lower parts. Brittleness is more dominant than deformation. It is the zone where the mineralization is most intensely observed together with the cataclasites. The breccia levels close to cataclasites have been intensively silicified and affected by hydrothermal alteration. The silicified breccia zone contains fluorite, disseminated pyrite, pyrite veinlets, and realgar, orpiment veinlets (Figure 3b). Some levels intensely contain Fe-oxide (limonite).

Slightly silicified marble breccias (averagely 1.00 m) are present in areas close to the marble contact of the Kayaköy formation (footwall) (Figure 3a-b).

3. Mineralization

Mineralizations in the study area and around are observed in three different locations; west of Kuz Hill, south of Kuz Hill, and Dalavihami Hill (Figure 2). Mineralizations are intermittently observed along the NW-SE direction on the low-angle normal fault zone of approximately 11 km length (Figure 2). West of Kuz Hill and Dalavihami Hill are the outcrops where mineralizations are best observed. The Dalavihami Hill mineralizations observed along the fault plane at approximately 2 km length and 0.20-22 m thickness constitute the subject of this study (Figure 4a). The hanging wall of the low-angle normal fault is occasionally eroded at the intersections and the ore can be traced directly on the marbles (Figure 4b). Drilling activities have shown that mineralizations are approximately 1.5 km in the N-S direction, 1 km in the E-W direction, and averagely 4 m in thickness (Yıldırım et al., 2019; figure 4a-b).

The mineralizations are associated with the low-angle normal fault which is between the Mid Late Triassic-Late Cretaceous aged Kayaköy formation and the Late Cretaceous Karaböğürtlen formation of the Bodrum nappe (Figure 4a-b) and they have not been affected by metamorphism.

The ore facies consists of breccia and cataclasite, and the mineralizations are mostly limited with silicified breccia and overlying cataclasites (Figure 4b). The predominant alteration is intense silicification and pyrite alteration. While pyrites are generally in the form of clusters and dissemination, they can also be observed as thin bands in cataclasites. Breccia grain size increases from the cataclasites to the marble breccias below. The thicknesses of cataclasites (0.20-9.30 m) and breccias (0.40-7.80 m) are approximately the same (Figure 3a and 4b). Trachy-latites/trachy-andesites are approximately 2 m in thickness and generally have a close spatial relationship with the mineralizations (Figure 3 and 4b). The sub-volcanic rocks are common in the cataclasites and breccia zone and are rarely observed as sills through the schists forming the hanging wall (Figure 3b). Sills are generally poorly mineralized.

Ore microscopy studies have shown that sulfide concentrations predominantly consist of pyrite, chalcopyrite, and sphalerite in descending order. Pyrites are very fine-grained, subhedral, anhedral, and cataclastic (Figure 5d, e). Trace amounts of bacteria (fromboidal) are observed in pyrite (Figure 5f). Pyrites show transformation into limonite (Figure 5g-i) and marcasite (Figure 5d, e) along with the fractures and cracks. Pyrite inclusions in limonites indicate transformation from pyrite. Au, observed along the fractures as little bubbles and discrete particles within the pyrite grains. Trace amounts of chalcopyrite and sphalerite are anhedral, fine-grained, and interlocked within the gangue minerals (Figure 5e). Organic matters are observed between gangue minerals and fractures under a microscope. They are mostly clustered within limonites (Figure 5h, i). It has been determined that organic matter is semi-graphite.

Gold mineralization is associated with silicification and pyrite. The predominant sulfide mineral is pyrite containing a trace amount of chalcopyrite and sphalerite. Transformation to limonite and a small amount of hematite are observed in pyrites. Gold

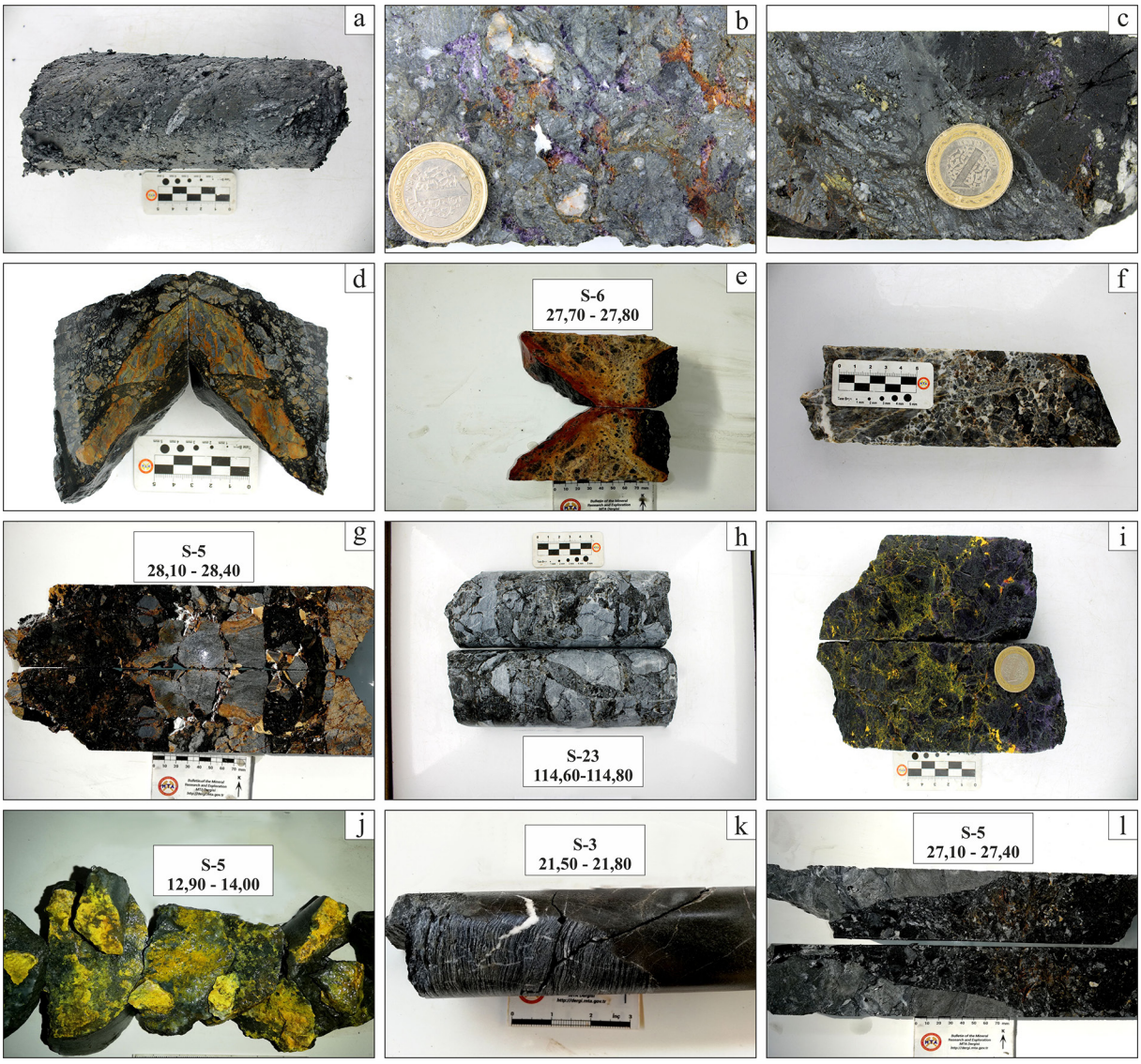

Figure 6- a) Euhedral, biaxially sliced hornblende crystals and opacitized biotites in trachy-latite/trachy-andesite, b) microlitic texture, c) sanidine phenocrystal showing carlsbad twinning, observed in microporphyric textured trachytes, d) euhedral pyrite showing transformation to marcasite, e) pyrite and trace amounts of anhedral sphalerite and chalcopyrite, f) pyrite in the form of bacteria (framboidal), g) widespread limonitization in silicified breccia zone, h) non-mineralized, i-j) florite staining and organic matter (semi graphite) between crack and gague minerals and at the grain boundaries, k) cataclastics and l) tarchy-latite cutting silisified.

might be transported as bisulfite complexes. Fluorite is mostly in thin quartz-fluorite veinlets and the form of space-filling (Figure 6b, i). Besides, realgar and orpiment occurrences are mostly observed as staining in the fracture zones of trachy-latite/trachy-andesites (Figure 6i, j) and sometimes in cataclasite and breccia.

3.1. Hydrothermal Alteration

Alterations defined in the mineralization area are; (I) silica replacements/veinlets and (II) quartz-pyrite replacements/veinlets.

Cataclasites with intense organic matter, containing fluorite, pyrite matrix, and mostly schist-quartz fragments just below the fault gauge (Figure 6a) and are poorly silicified (Figure 6b-c). Limonitization/ hematitization (transformation from pyrite) is common through some of the levels (Figure 6d).

The most common alteration is silica replacement, which is often associated with high-grade gold mineralization. Silicification is mostly in breccias and is cut-cross by limonite vein/veinlets (Figure 6f). Silicified parts are sometimes overlain by limonite

(Figure 6e). Thin quartz veins cutting the silicification irregularly are observed. Silica replacement/veinlets are observed as matrix replacement within the breccia and partial absorption is observed in the breccia fragments (Figure 6g). The colour of silica ranges from dark-gray to light-gray. Dark-gray parts contain <1-2 % fine-grained disseminated pyrite. Very high gold grades are in the dark-gray silicified parts with iron-oxide staining. This zone passes into the less silicified and organic matter-rich cataclasite zone at the top and the non-mineralized marble breccia at the bottom (Figure 6h).

Quartz-pyrite alteration usually occurs in the breccia zone as a gray-green matrix replacement and quartz veins often cut-cross the altered matrix. Pyrites are usually localized in veins and are less common. Quartz-pyrite alteration transitions dark-gray silicification towards upper levels and marble breccia towards lower levels. This alteration can be distinguished from trachy-latite/trachy-andesites by the absence of feldspar phenocrystals. Apart from the silica replacement, it is the second important type of alteration for gold mineralization.

Hydrothermal alterations and associated minerals can be observed both laterally and vertically. While the most intense silicification is in the breccias of the fault zone, it is much less in the cataclasites. The fault gauge is not silicified.

4. Analytical Techniques

Chemical analyses of thirty seven rock samples collected from the mine area including drill cores, made in MTA (General Directorate of Mineral Research and Exploration) laboratories. Drill cores with ore were sampled at onemeter intervals. The sampling procedure was completed according to standards recommended by international organizations like Crirsco (Committee for Mineral Reserves International Reporting Standards) and JORC (Joint Ore Reserve Committee, Australia). The most characteristic samples were chosen from the data set and are presented as a table 1 in the article. Four fault gauge samples, ten cataclasite samples, eight trachy-latite/trachy-andesite samples, ten silicified breccia samples and five marble breccia samples were selected for whole rock analyses using lithium metaborate/tetraborate fusion ICP for SiO_2, Al_2O_3, TiO_2, Fe_2O_3(T), K_2O, Na_2O, CaO, MgO, MnO and P_2O_5.

5. Geochemistry

In the field of mineralization, the analysis of the samples obtained from the drillings carried out by MTA for exploration and reserve studies have revealed high Au values, but base metal concentrations are insignificant (Figure 7). Both detailed geological studies and drilling studies have indicated new data in the field of mineralization and have revealed the economic importance of gold mineralization in buried areas. The chemistry of the ore, host rocks (Table 1) and even drill core samples have contributed to identify and classify the mineralization.

The element concentrations of the low-angle normal fault zone containing the gold mineralization are high in silicified breccias, cataclasites, and trachy-latites, but much lower in fault gauge and marble breccias (Figure 7; table 1). The concentrations of the main units are: Fault gauge 21-31 ppm Cu, 27-76 ppm Zn, <1 ppm Ag, 25-125 ppb Au, 239-1199 ppm As, 5-19 ppm Sb, %<0.01-0.11 F; cataclasite 11-28 ppm Cu, 41-495 ppm Zn, <1-15.5 ppm Ag, 790-3500 ppb Au, 899-5976 ppm As, 25-171 ppm Sb, %1.6-11,0.50 F; silicified breccia 11-23 ppm Cu, 12-185 ppm Zn, <1-3.4 ppm Ag, 850-6300 ppb Au, 105-3996 ppm As, 6-103 ppm Sb, %<0.01-0.8 F; trachy-latite/trachy-andesite 11-28 ppm Cu, 7-264 ppm Zn, <1-21 ppm Ag, 1000-4800 ppb Au, 895-11577 ppm As, 23-293 ppm Sb, %<0.01-0.5 F; marble breccia <3-7 ppm Cu, 21-470 ppm Zn, <1 ppm Ag, 110-210 ppb Au, 100-431 ppm As, <5-12 ppm Sb, %<0.01 F.

6. Discussion and Results

Yeşilyurt gold mineralization has developed as part of the silicification and quartz-pyrite alteration hosted by the low-angle normal fault zone. Mineralization is polymetallic, which is related to gold deposits associated with silver, arsenic, and fluorite as well. A simple genetic model of mineralization can be developed by discussing the origin of the fault zone and the origin of the subsequent hydrothermal system. This genetic model may give an idea about the mineralization associated with the extensional environment in the Eastern Taurus.

6.1. Origin of the Fault Gauge

The main structural elements in the mineralization area are the low-angle normal fault as well as the

Table 1- Compositional data of the samples from low-angle normal fault zone, Yeşilyurt gold mineralization.

	Sample	Au (ppb)	Ag (ppm)	As	Bi	Co	Cu	Mo	Ni	Pb	Sb	V	Zn	F (%)	Au/Ag (ppm)
Fault Gauge	S-11-21	25	<1	279	<5	7	31	<5	28	9	5	5	76	<0.01	0.03
	S-14-20	125	<1	1023	<5	7	28	<5	73	8	7	5	27	<0.01	0.13
	S-16-07	60	<1	239	<5	<5	21	<5	133	9	5	5	48	<0.01	0.06
	S-16-09	55	<1	1199	<5	9	26	<5	199	14	19	<5	60	0.11	0.06
Cataclasite	S-17-03	3500	15.5	2370	<5	<5	20	69	54	95	134	53	151	5.71	0.23
	S-94-22	3200	6.5	2657	<5	8	28	31	78	27	32	60	495	2.09	0.49
	S-17-04	2205	8.8	1672	<5	5	26	58	300	94	67	47	132	4.81	0.25
	S-17-02	2200	6.8	1878	<5	8	22	18	56	28	75	33	125	2.80	0.32
	S-08-08	1560	<1	3379	<5	<5	21	14	96	25	104	55	297	1.80	1.56
	S-08-07	1080	2.1	2695	<5	6	18	14	46	19	64	37	70	1.60	0.51
	S-08-06	1040	2.2	5976	<5	8	18	22	129	35	171	44	186	1.88	0.47
	S-02-02	985	<1	1198	<5	<5	16	17	244	49	39	56	52	11.50	0.99
	S-02-01	905	<1	1922	<5	<5	11	19	177	51	41	49	44	4.50	0.91
	S-02-03	790	<1	899	<5	<5	12	34	41	46	25	38	41	4.60	0.79
Trachy-latite/trachy-andesite	S-46-29	4800	21.0	2143	<5	<5	12	95	26	12	293	35	22	0.01	0.23
	S-46-28	3700	9.9	11577	<5	<5	15	38	23	14	225	36	33	0.01	0.37
	S-46-31	3100	16.7	8797	<5	5	17	42	41	21	60	89	264	0.20	0.19
	S-46-30	2900	17.7	895	<5	<5	13	50	32	13	62	50	7	0.01	0.16
	S-80-54	1700	6.1	2522	<5	11	28	12	79	20	38	13	84	0.20	0.28
	S-20-41	1400	<1	1707	<5	<5	20	31	25	15	41	28	164	0.01	1.40
	S-46-32	1350	7.7	5143	<5	<5	11	15	23	12	23	45	148	0.50	0.18
	S-20-42	1000	<1	964	<5	<5	20	21	31	19	27	19	112	0.40	1.00
Silicified breccia	S-37-13	6300	1.5	998	<5	<5	23	11	9	5	24	14	28	0.01	4.20
	S-37-14	6100	<1	2093	<5	<5	11	15	8	5	65	52	38	0.01	6.10
	S-14-24	3300	1.1	1423	5	5	22	12	365	13	53	32	140	<0.01	3.00
	S-05-19	2390	3.4	2478	6	17	21	7	233	22	53	11	33	0.01	0.70
	S-44/1-07	2050	2.3	1556	<5	5	23	31	56	90	103	71	88	0.01	0.89
	S-83-11	2015	1.0	3996	<5	6	15	11	26	<5	20	31	185	0.80	2.02
	S-44/1-06	1835	1.8	951	<5	5	22	26	21	81	31	52	12	0.60	1.02
	S-05-18	1140	3.0	1628	<5	10	15	16	469	31	27	14	37	0.01	0.38
	S-05-21	955	2.3	1167	<5	17	21	5	228	11	26	11	28	0.03	0.42
	S-90/1-10	850	<1	105	<5	<5	11	18	17	8	6	16	167	0.50	0.85
Marble breccia	S-57-36	210	<1	184	<5	<5	7	18	5	5	12	19	141	<0.01	0.21
	S-73-35	170	<1	431	<5	<5	3	6	19	20	5	23	276	<0.01	0.17
	S-22-18	130	<1	167	<5	<5	4	7	7	7	10	31	470	<0.01	0.13
	S-29/1-36	110	<1	423	<5	<5	<3	<5	5	<5	<5	12	21	<0.01	0.11
	S-57-35	110	<1	100	<5	<5	<3	<5	<5	<5	6	9	81	<0.01	0.11

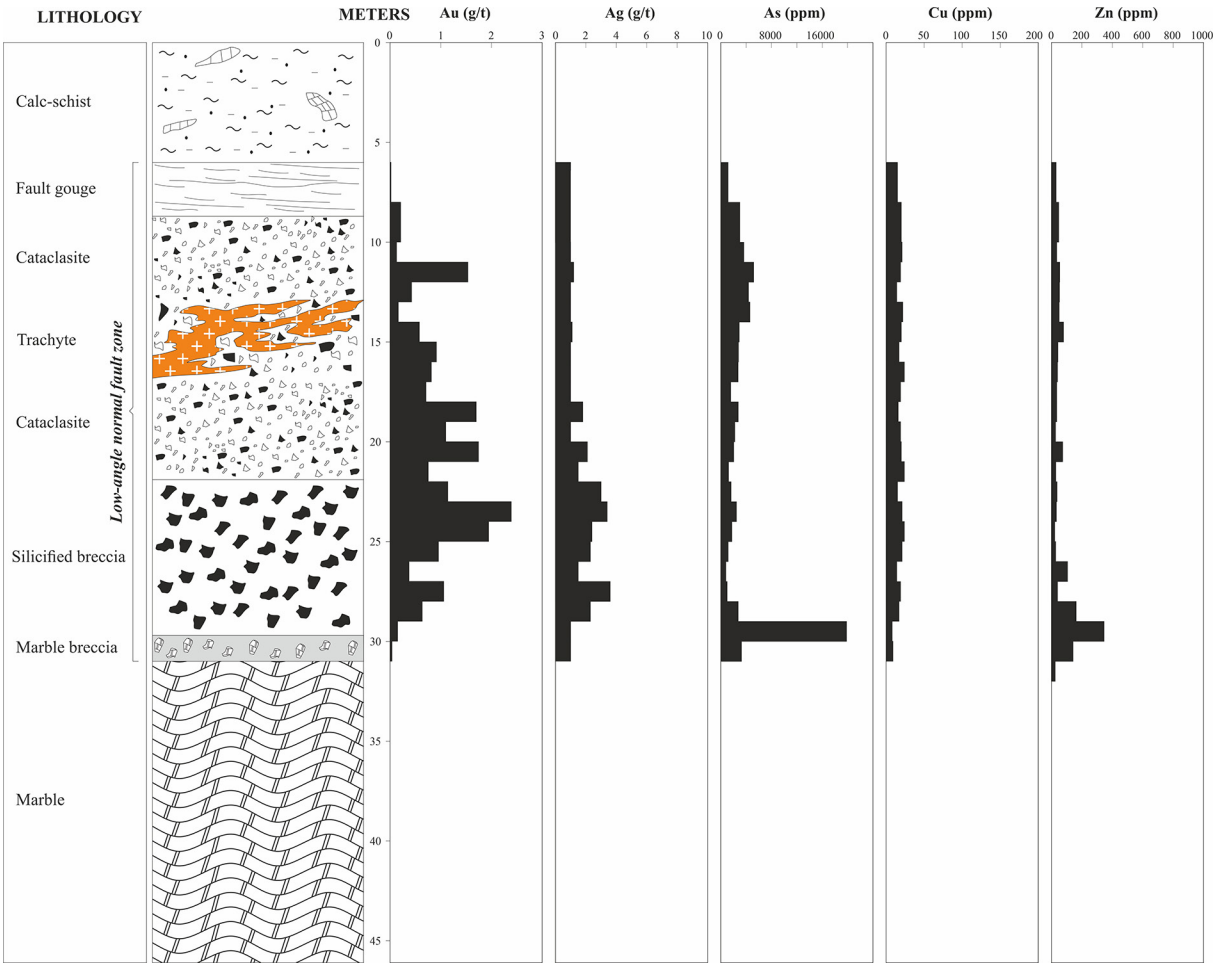

Figure 7- Graphical log of the S-5 drilling shown in figure 4. Gold, silver, arsenic, copper, and zinc contents of the low-angle normal fault zone and main lithological units are shown (Sample intervals of 1 meter; modified from Yıldırım et al., 2019).

reverse and strike-slip faults. The region is located in a tectonically active environment. It is known that the compressive tectonic regime has been active especially during the Late Cretaceous-Paleogene-Neogene (?) period (Şengör and Yılmaz, 1981). The low-angle normal fault must have developed in the Paleogene-Neogene (?) period, with the active role of an extensional tectonic environment. During this period, it is thought that thrust faults within the metamorphic core complex have reactivated as normal faults. Paleogene-Neogene (?) extensional tectonics is associated with back-arc extension and/or subduction rollback. During this period, small-volume of felsic magmas (trachy-latite/trachy-andesite) have settled in shallow crust levels along the low-angle normal fault.

The suggestions about detachment like faulting on Yeşilyurt gold mineralization are based on local and regional observations. The most important arguments; (I) existence of fault gauge, (II) asymmetric folding on cataclasites and relatively silicified breccias just below fault gauge, and (III) evidence showing that the faulting is partially coincident with the emplacement of the trachy-latite/trachy-andesite intrusions.

The fault gauge zone always separates the hanging wall schists from the footwall marbles. The fault presents a braided structure due to surface erosion. The fault gauge along these inter-sections have moved away from the environment after this erosion, which has made mineralization reveal. Asymmetrical folds have been observed in the cataclasites and breccias underlying the fault gauge. The down-dipping parts of the folds are slightly steeper and increase the possibility of normal faulting and displacement. Also, high-grade extensional shear textures and low-grade fault gauge and breccias support this situation as well.

The emplacement of Paleogene-Neogene (?) sub-volcanic sills and dykes appears to be simultaneous with low-angle faulting. Local and regional geological evidence suggest that the fault zone in the mineralization area indicates an origin of detachment faulting within extensional tectonism during the Paleogene-Neogene (?) period.

Mineralization is observed within the zones which have been heavily silicified and brecciated at the same time of faulting. Also, alterations and mineralizations overlying the cataclastic textures indicate that post-faulting processes in the ore deposit have been also effective. However, there is also evidence for post-mineralization faulting. Deformed pyrites can be an example of this.

6.2. Geochemical Characteristics of Mineralization Associated with Low-Angle Normal Fault

Element (Au, Ag, Pb, Zn, Sb, Mo, F, As) distributions were studied to understand the relationship between low-angle normal fault and mineralization. Correlation coefficients between minor elements and enrichment coefficients were calculated (Table 2). The mineralization factors reflect a strong positive correlation of gold against silver, antimony, and molybdenum (0.48, 0.50, 0.51; table 2, 8a-c), while weaker positive correlation against arsenic (0.34; figure 8d). A relatively negative correlation of gold against Zn and Cu (-0.08, 0.15; figure 8e, f) was observed. The Gold/Silver ratio is between 0.16 and 6.1 (Table 1).

Fluorites are observed in the mineralization area within the fault zone and gold concentrations in these zones are relatively higher. Fluor values are in the range of 0.01-11.5% (Table 1; average 1.59%), and they are considered to be economically insignificant. However, they might be recovered as a by-product. The source of high arsenic values in the ore zone (Table 1; mean 0.27%) are realgar and orpiment.

Geochemical data may have the following consequences:

I. Low-angle normal fault zone provides permeable fluid channel which is necessary for precipitation of minerals from hydrothermal fluids. Organic materials, creates suitable reduced setting for precipitating of sulfides. Therefore, high concentrations of Au and As may be associated with faulting processes. Most of the possible gold mineralizations in the region must be in the detachment fault zone.

II. Au and Ag have a weak positive correlation with other elements such as F, Mo, Sb. This may indicate that it is part of polymetallic mineralization and may suggest the element assemblage of deposits to be discovered in the area.

III. The higher concentrations of Au, Ag, and As in the center of the low-angle normal fault zone and

Table 2- Correlation coefficients between analyzed elements.

	Au	Ag	As	Bi	Co	Cu	Mo	Ni	Pb	Sb	V	Zn	F
Au	1.00	0.49	0.34	0.07	-0.09	0.15	0.49	-0.08	0.07	0.51	0.40	-0.08	-0.03
Ag		1.00	0.42	-0.02	-0.08	0.02	0.83	-0.11	0.18	0.62	0.43	-0.01	0.04
As			1.00	0.02	-0.01	0.06	0.26	-0.06	0.00	0.55	0.45	0.12	-0.03
Bi				1.00	0.59	0.08	-0.13	0.21	-0.02	0.00	-0.18	-0.12	-0.09
Co					1.00	0.34	-0.29	0.43	-0.12	-0.09	-0.37	-0.15	-0.16
Cu						1.00	0.02	0.29	0.27	0.04	-0.01	-0.08	0.06
Mo							1.00	-0.09	0.45	0.72	0.51	-0.03	0.23
Ni								1.00	0.24	-0.05	-0.09	-0.16	0.25
Pb									1.00	0.22	0.53	-0.04	0.55
Sb										1.00	0.37	-0.10	0.07
V											1.00	0.32	0.39
Zn												1.00	0.001
F													1.00

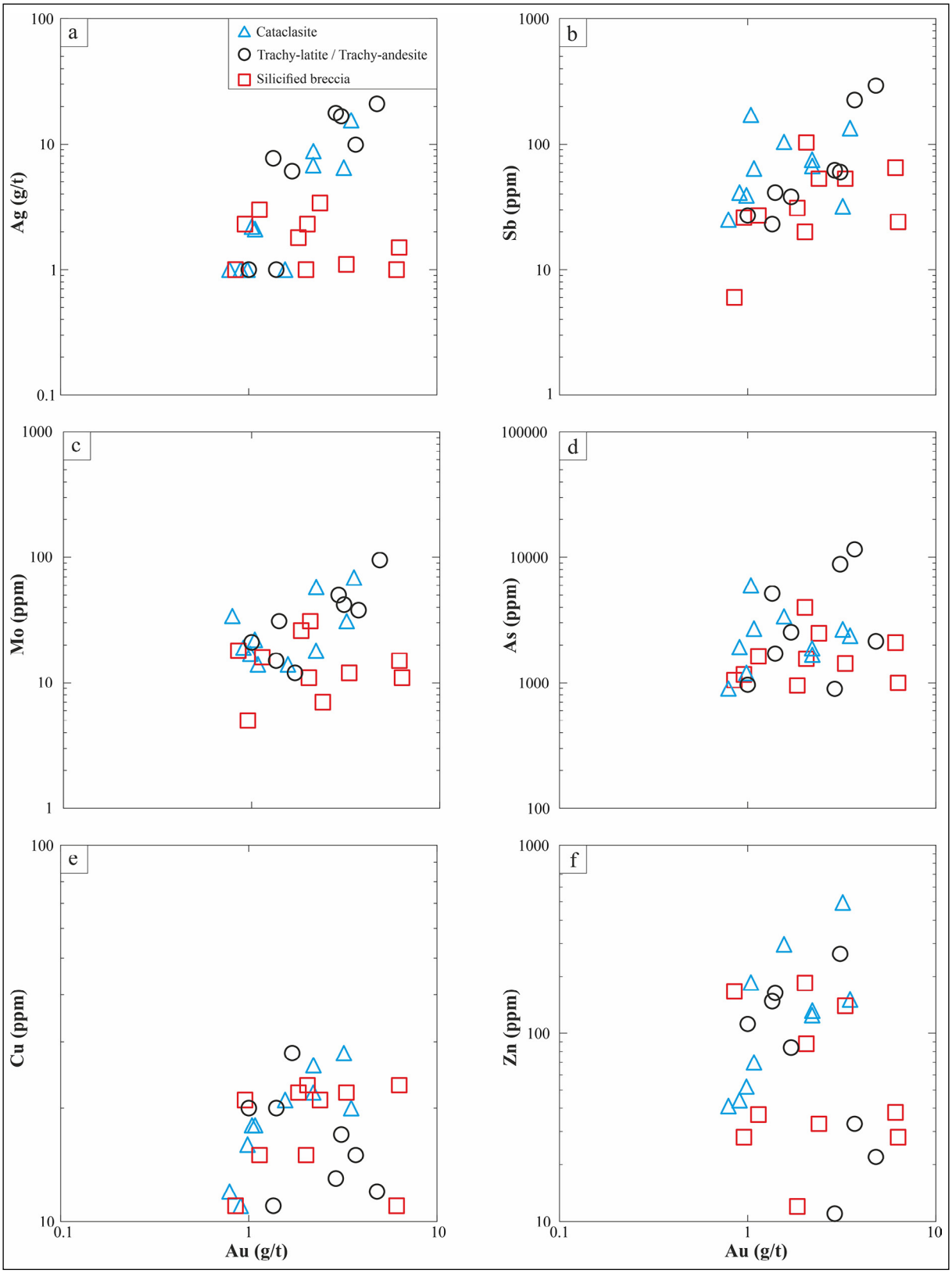

Figure 8- Binary variation diagrams against gold versus a) Ag, b) Sb, c) Mo, d) As, e) Cu and f) Zn. Compositional distributions of cataclasite (blue triangle), trachy-latite/trachy-andesite (empty circle), and silicified breccia (red square) of Yeşilyurt mineralizations.

lower towards the edges of the fault zone may indicate higher permeability and/or organic material. When geochemical data are combined with detailed geology, it gives the idea that this area is important in terms of Au, Ag, and As mineralizations. Therefore, the researches over the region should be continued.

6.3. Mineralization Genesis and Genetic Model

The origin of the fluids causing Yeşilyurt gold mineralization is currently not well understood. Trachy-latite/trachy-andesites exposed to intense sericite and carbonate alteration are directly associated with the ore and there is no age data. The spatial relationship of these rocks with the ore and the association of gold, fluorite, realgar, orpiment, and sulfide suggest that they have a genetic relationship with Paleogene-Neogene (?) magmatism.

Metal-containing fluids should have precipitated sulfides in a relatively low-temperature/low-pressure environment along the low angle fault zone (cataclasite and breccia) in the Yeşilyurt mineralization area. The erosion of the low angle fault zone caused erosion of the hanging wall itself as well. This situation has made the mineralization exhume to be discovered.

The presence of brecciated, folded, and undisturbed quartz veins on the surface indicates faulting is a part of syn-mineralization. The presence of pyrite, fluorite, realgar, and orpiment together with breccia and cataclasites also suggest syn-mineralization.

Yeşilyurt gold mineralization is located along an unusual regional detachment/low-angle normal faultandit is the first gold deposit associated with a low-angle normal fault identified in the eastern Taurus orogenic belt. This mineralization will lead to the discovery of a new gold deposit belt along the Eastern Taurus orogenic belt.

6.4. Gold Deposits Associated with Detachment Faults

Different types of mineralization observed in low-angle detachment faults associated with metamorphic core complexes have mostly been described in the southwestern USA. Most of the studies have been in the Arizona Geology Survey. These deposits include Piacho (Drobeck et al., 1986; Liebler, 1988), Bullard Peak (Roddy et al., 1988), southwestern Arizona; Cyclopic (Myers and Smith, 1986), northwestern Arizona; Riverside Pass (Wilkinson et al., 1988), Whipple-Buckskin-Rawhide (Spencer and Welty, 1986), Mesquite (Manske et al., 1988) southeastern California; San Luis (Benson and Jones 1996), Colorado. Apart from these deposits, Kokanee Range (Beaudoin et al., 1991) British Colombia; Luolin-Henan (Dai and Haiyang, 2005), China; Ada Tepe (Marchev et al., 2004), Bulgaria; Ernesto-Lavrinha (Puritch et al., 2016) and Brazilian deposits are examples of this mineralization type.

Such beds are divided into two categories by Eng et al., (1995) as base metalliferous (Whipple-Buckskin-Rawhide and Kokanee) and base-metal-poor (Picacho, Riverside Pass, Ada Tepe, and San Luis) deposits. Base-metal-poor deposits can be interpreted as detachment fault-controlled low-sulfidation gold mineralization. Mineralizations are in the form of massive, tabular ore bodies within the fault zone and they are open-space ore filling type in listric faults (Zappettini et al., 2017). Ores are observed in the areas showing intense silicification and brecciation taken place simultaneously with the detachment fault.

Quartz and fewer calcite minerals are the main gangue minerals in Yeşilyurt gold mineralization which has many common features with base-metal-poor gold deposits such as the presence of gold as tabular ore body in shallow-dipping detachment fault, quartz-pyrite and silica replacements and veinlets, limonite-hematite (transformation from pyrite) developed as supergene and also low base metal and low Au/Ag (average 1.07) content. On the other hand, the characteristics of the mineralization reveal some notable differences with the presence of common fluorite, realgar-orpiment (high As content), semi-graphite, and bacterial pyrite despite the lack of copper, specular hematite, and adularia, compared to the base-metal poor mineralizations associated with detachment faults. Besides, the lack of adularia which indicates the epithermal mineralization with low sulfidation and boiling of neutral pH solution, is an important factor that separates this deposit from epithermal system. In addition to these, syn-tectonic magmatic rocks defined along the detachment fault in the mineralization area have a genetic relationship with the ore and these syn-tectonic magmatic rocks have also been described in different areas around the world (Reynolds and Lister, 1987).

Yeşilyurt gold mineralization with its distinctive structures and differences is the first gold deposit associated with a low-angle normal fault in the region and country. Besides, the correlation between base metalliferous deposits associated with the low-angle normal fault and the stratigraphical and structural position and mineralization assemblage of the Cafana (Görgü)-Malatya Pb-Zn mineralization located in the north of the studied area can bring a new perspective to mineral exploration in the region.

Acknowledgments

This study was carried out as a part of MTA project titled "Maden Karmaşığı Polimetal Maden Aramaları (2018/2020-32-13-01-1)", affiliated to the General Directorate of Mineral Research and Exploration, Department of Mineral Research and Exploration. We would like to thank Geological Engineer (MSc.) Mahmut Eroğlu and Geological Engineer Turan Bengin who contributed to the field studies, Geological Engineers Tahsin Aksoy and Füsun Niğdeli (Feasibility Department), who estimated the reserve of the mineralization, and the Geological Engineer Yunus Sönmez for the revision of the figures in the article. Last but not least, we would like to thank all the MTA team. We also thank Ali Sholeh for his constructive criticism and suggestions.

References

Akıncı, O.T. 2009. Ophiolite-hosted copper and gold deposits of southeastern Turkey: formation and relationship with seafloor hydrothermal processes. Turkish Journal of Earth Sciences 18, 475–509.

Altman, K., Liskovich, M. 2011. Çöpler Sulfide Expansion Project prefeasibility study, Erzincan province, Turkey: Canadian National Instrument 43-101 Technical Report 176.

Altuncu, S. 2009. Türkiye Fluorit Yataklarının Karşılaştırmalı İncelenmesi. Doktora Tezi, İstanbul Üniversitesi, Fen Bilimleri Enstitüsü, 147 (unpublished).

Asutay, H. J., Turan, M., Poyraz, N., Orhan, H., Tarı, E.,Yazgan, E. 1986. Doğu Toroslar Keban-Baskil (Elazığ) Dolaylarının Jeolojisi. Maden Tetkik ve Arama Genel Müdürlüğü, Rapor No: 8007, Ankara (unpublished).

Beaudoin, G., Taylor, B.E., Sangster, D.F. 1991. Silver-lead-zinc veins, metamorphic core complexes, and hydraulic regimes during crustal extension. Geology 19, 1217–1220.

Bedi, Y., Yusufoğlu, H. 2018. 1/100.000 scale Turkish Geological Maps, Malatya-L40 Quadrangle, No: 261, Publication of General Directorate of Mineral Research and Exploration 89. (in Turkish with English Abstract).

Benson, R. G., Jones, D.M. 1996. Geology of the San Luis gold deposit, Costilla County, Colorado; an example of low-angle normal fault and rift-related mineralization in the Sangre De Cristo Range of Colorado. Special Publication - Colorado School of Mines

Çelebi, H. 2009. Türkiye apatitli manyetit yatakları: jeolojisi, jeokimyası ve ekonomik potansiyeli. İstanbul Yerbilimleri Dergisi 22, 1, 67-83.

Dai, T.G., Haiyang Z. 2005. The relationship between detachment faults and mineralization in Luolin district, Henan, China Mineral Deposit Research: Meeting the Global Challenge 909-911

Drobeck, P.A., Hillemeyer, J.L., Frost, E.G., Liebler, G.S. 1986. The Picacho Mine: a gold mineralized detachment in southeastern California. In: Beatty, B. and Wilkinson, P.A.K. (eds): Frontiers in geology and ore deposits of Arizona and the Southwest. Arizona Geological Society Digest. XVI, Tucson, 187–221.

Dumanlılar, H.D., Aydal, D., Dumanlılar, O. 1999. Geology, mineralogy and geochemistry of sulfide mineralization in the İspendere region (Malatya). Bulletin of the Mineral Research and Exploration 121, 225–250.

Eng, T., Boden D.R., Reischman, M.R., Biggs, J.O. 1995. Geology and mineralization of the Bullfrog Mine and vicinity, Nye County, Nevada. In: Coyner, A.R. and Fahey, P.L. (eds.): Geology and ore deposits of the American Cordillera. Symposium Proceedings, Geological Society of Nevada, Reno/Sparks, Nevada. 1, 353–400.

Gözübol, A.M., Önal, M. 1986. Çat Barajı İsale tünelinin mühendislik jeolojisi ve kaya mekaniği incelemesi ve Malatya-Çelikhan alanının jeolojisi. TÜBİTAK, TB AG-647, Ankara.

Hanelçi, Ş., Çelebi H. 2013. Geology and petrology of igneous rocks of the Zeryandere Lagerstaettendistriktes Keban, Elazığ Province, Turkey. Journal of Geology Sciences 41/42 (5-6), 301-315.

Helvacı, C., Griffin, W.L. 1984. Rb-Sr geochronology of the Bitlis massif, Avnik (Bingöl) area, SE Turkey. In: Dixon, J.E. and Robertson, A.H.F. (eds). Geological Evolution of the Eastern Mediterranean. Special Publication of the Geological Society of London 17, 403-413.

İmer, A., Richards, J.P.,Creaser, R.A. 2012. Age and tectonomagmatic setting of the Eocene Çöpler-Kabatas¸ magmatic complex and porphyryepithermal Au deposit, East Central Anatolia, Turkey. Mineralium Deposita 48, 557–583

Kalender, L. 2011. Oxygen, carbon and sulfur isotope studies in the Keban Pb-Zn deposits, eastern Turkey: an approach on the origin of hydrothermal fluids. Journal of African Earth Sciences 59 (4-5), 341–348.

Kalender, L., Kırat, G., Bölücek, C., Sağıroğlu, A. 2009. Görgü (Malatya-Turkiye) Pb-Zn Cevherleşmelerinin Eski İmalat Pasalarının Jeokimyası, 62. Jeoloji Kurultayı, Ankara.

Ketin, İ.1983. Türkiye Jeolojisine Genel Bir Bakış: İTÜ Kütüphanesi, Sayı 1259, 595

Kipman, E. 1981. Keban'ın jeolojisi ve Keban şaryajı İstanbul Üniversitesi Yerbilimleri Dergisi 1(1-2), 75-81.

Kuşcu, İ., Yılmazer, E., Demirela, G. 2007. Iron oxide-copper±gold deposits in Turkish Tethyan collage: Society for Geology Applied to Mineral Deposits (SGA), roceedings of the 9th Biennial SGA Meeting, Dublin, 853–857.

Kuşcu, İ., Gencalioğlu-Kuşcu, G., Tosdal, R.M., Ullrich, T., Friedman, R., 2010. Magmatism in the Southeastern Anatolian orogenic belt: transition from arc to postcollisional setting in an evolving orogen. Geological Society, London, Special Publications 340, 437–460.

Kuşcu, İ.,Tosdal R.M.,Gencalioğlu Kuşcu, G., Friedman, R., Ullrich,T.D. 2013. Late Cretaceous to Middle Eocene magmatism and metallogeny of a portion of the Southeastern Anatolian orogenic belt, East-Central Turkey. Economic Geology 108 (4), 641-666

Liebler, G.S.1988. Geology and gold mineralization at the Picacho mine, Imperial County, California. In: Schafer, R.W., Cooper, J.J., Vikre, P.G. (eds): Bulk mineable precious metal deposits of the Western United States, Symposium Proceedings, Geological Society of, Reno/Sparks, Nevada. Part IV, Gold-silver deposits associated with detachment faults, 453–504.

Long, K.R. 1992. Preliminary descriptive deposit model for detachment-fault-related mineralization. In: Bliss, J. (Ed.), Developments in Mineral Deposit Modeling. U.S. Geological Survey Bulletin 2004, 52-56.

Manske, S.L., Matlack, W.F., Springett, M.W., Strakele, A.E., Jr, Watowich, S.N., Yeomans, B., Yeomans, E. 1988. Geology of the Mesquite deposit, Imperial County, California. Mining Engineering 40, 439-444.

Marchev, P., Raicheva, R., Downes, H., Vaselli, O., Massimo, C.,Moritz, R. 2004. Compositional diversity of Eocene-Oligocene basaltic magmatism in the Eastern Rhodopes, SE Bulgaria: implications for its genesis and geological setting. Tectonophysics 393, 301–328

MTA, 2002. 1:500.000 scale geology map of Turkey. General Directorate of Mineral Research and Exploration (Turkey), Ankara, Turkey.

Myers, I.A., Smith, E.I. 1986. Control of gold mineralization at the Cyclopic mine, Gold Basin district, Mohave county, Arizona. Economic Geology 81, 1553-1557.

Okay, A.I. 2008. Geology of Turkey: A Synopsis. Anschnitt 21, 19-42.

Özgül, N. 1976. Toroslar'da bazı temel jeoloji özellikleri. TJK Bülteni 19, 65-78

Öztürk, H., Hanilçi, N., Altuncu, S., Kasapçı, C. 2019. Rare Earth Element (REE) resources of Turkey: an overview of their formation types. Bulletin of the Mineral Research and Exploration 159, 127–141.

Puritch, E., Bradfield, A., Routledge, R., Sutcliffe, R., Burga, D., Barry, J., Cornejo, F., Batelochi, M., Lister, D. 2016. Technical Report and updated Resource Estimate on the EPP Project. Mato Grosso, Brazil. Aura Minerals Inc. NI 43-101 & 43 - 101F1 Technical Report.

Revan, M.K.,Genç, Y. 2003. Malatya-Yeşilyurt altınlı fluorit cevherleşmesi: Toroslarda paleokarst tipi bir yatak. Jeoloji Mühendisliği Dergisi 27/2, 76-93.

Reynolds, S.J., Lister, G.S. 1987. Structural aspects of fluid-rock interactions in detachment zones. Geology 15, 362-366.

Robertson, A.H.F., Boulton, S.J., Taslı, K., İnan, N., Yıldırım, N., Yildiz, A., Parlak, O. 2016*a*. Late Cretaceous-Miocene sedimentary development of the Arabian continental margin in SE Turkey (Adıyaman Region): implications for regional palaeogeography and the closure history of Southern Neotethys. Journal Asian Earth Science 115, 571-616

Robertson, A.H.F., Parlak, O., Yıldırım, N., Dumitrica, P., Taslı, K. 2016*b*. Late Triassic rifting and Jurassic–Cretaceous passive margin development of the Southern Neotethys: evidence from the Adıyaman area, SE Turkey.International Journal of Earth Sciences 105,167–201

Roddy, M.S., Reynolds, S.J., Smith, B.M., Ruiz, J. 1988. K-metasomatism and detachment-related

mineralization, Harcuvar Mountains, Geological Society of America Bulletin 100 (10), 1627-1639.

Sağıroğlu, A. 1988. Cafana (Görgü) Malatya karbonatlı Zn-Pb yatakları. Cumhuriyet Üniversitesi Mühendislik Fakültesi Dergisi Seri A, 5(1), 3-13.

Spencer, J.E., Welty, F.W. 1986. Possible controls of base- and precious-metal mineralization associated with Tertiary detachment faults in the lower Colorado River through, Arizona and California. Geology 14, 195-198.

Şaşmaz, A., Önal, A., Önal, M. 1999. Çelikhan (Adıyaman) fluorit cevherleşmeleri ve bunların NTE jeokimyası. I. Batı Anadolu Hammadde Kaynakları Sempozyum Bildirileri, 378–387

Şaşmaz, A., Önal, A., Sağıroğlu, A., Önal, M., Akgül, B. 2005. Origin and nature of the mineralizing fluids of thrust zone fluorites in Çelikhan (Adıyaman, eastern Turkey): a geochemical approach. Geochem J 39, 131–139

Şengör, A.M.C.,Yılmaz, Y. 1981. Tethyan evolution ol Turkey: A plate tectonic approach. Tectonophysics 75,181 - 241.

Wilkinson, W.H., Wendt, C.J., Dennis, M.D. 1988. Gold mineralization along Riverside Mountains Detachment Fault, Riverside County, California. Bulk mineable precious metal deposits of the Western United States, Symposium Proceedings, Part IV, Goldsilver deposits associated with detachment faults Nevada, 487–504.

Yıldırım, E., Yıldırım, N., Dönmez, C., Koh, S., Günay, K. 2019. Mineralogy, rare earth elements geochemistry and genesis of the Keban-West Euphrates (Cu-Mo)-Pb-Zn skarn deposit (Eastern Taurus metallogenicbelt, E Turkey) Ore Geology Reviews 114 103102.

Yıldırım, N. 2013. Havza-kuşak madenciliği kapsamında keşfedilen "GD Anadolu Kıbrıs Tipi VMS Metalojenik Kuşağı": Koçali Karmaşığı, Adıyaman Bölgesi, Türkiye. Maden Tetkik ve Arama Genel Müdürlüğü Doğal Kaynaklar ve Ekonomi Bülteni 14, 47–55.

Yıldırım, N., İlhan, S., Yıldırım, E., Dönmez, C. 2012. The geology, geochemistry and genetical features of the Ormanbaşı Hill (Sincik, Adıyaman) copper mineralization. Bulletin of the Mineral research and exploration 144, 75–104.

Yıldırım, N., Dönmez, C., Kang, J., Lee, I., Pirajno, F., Yıldırım, E., Günay, K., Seo, J.H., Farquhar, J., Chang, S.W. 2016.A magnetite-rich Cyprus-type VMS deposit in Ortaklar: A unique VMS style in the Tethyan metallogenic belt, Gaziantep, Turkey. Ore Geology Reviews 79, 425-442.

Yıldırım, N., Eroğlu, M., Aksoy, T., Niğdeli, F. 2019. Malatya-Yeşilyurt-Şerefhan yöresindeki AR: 201100417 (ER: 3102513) no'lu IV. Grup ruhsat sahasına ait (Au) madeninin buluculuk talebine esas kaynak tahmin raporu. Maden Tetkik ve Arama Genel Müdürlüğü (unpublished).

Yılmaz, Y., Yiğitbaş, E., Yıldırım, M., Genç, Ş.C. 1992. Güneydoğu Anadolu metamorfik masiflerinin kökeni. Türkiye 9. Petrol Kongresi Bildirileri 296-306.

Yılmazer, E., Kuşcu, İ., Demirela, G. 2003. Divrigi A-B kafa cevherleşmeleri: Alterasyon zonları ve zonlanma süreçleri: Bulletin of the Geological Society of Turkey, 46,17–34.

Yiğit, Ö. 2009. Mineral Deposits of Turkey in Relation to Tethyan Metallogeny: Implication for Future Mineral Exploration. Economic Geology 104, 19-51.

Zappettini, E.O., Rubinstein, N., Crosta, S.Segal, S.J. 2017. Intracontinental rift-related deposits: A review of key models. Ore Geology Reviews 89, 594-608.